Title

Protein—protein interactions: developing small-molecule inhibitors/stabilizers through covalent strategies

Journal

Trends in Pharmacological Sciences, 44(7)

ISSN

0165-6147

Authors

Lucero, Bobby

Francisco, Karol R

Liu, Lawrence J

et al.

Publication Date

2023-07-01

DOI

10.1016/j.tips.2023.04.007

Peer reviewed

HHS Public Access

Author manuscript

Trends Pharmacol Sci. Author manuscript; available in PMC 2024 April 09.

Published in final edited form as:

Trends Pharmacol Sci. 2023 July ; 44(7): 474–488. doi:10.1016/j.tips.2023.04.007.

Protein–protein interactions: developing small-molecule inhibitors/stabilizers through covalent strategies

Bobby Lucero[1], **Karol R. Francisco**[2], **Lawrence J. Liu**[1], **Conor R. Caffrey**[2], **Carlo Ballatore**[3,*]

[1]Department of Chemistry and Biochemistry, University of California, San Diego, 9500 Gilman Drive, La Jolla, CA 92093, USA

[2]Center for Discovery and Innovation in Parasitic Diseases, Skaggs School of Pharmacy and Pharmaceutical Sciences, University of California, San Diego, 9500 Gilman Drive, La Jolla, CA 92093, USA

[3]Skaggs School of Pharmacy and Pharmaceutical Sciences, University of California, San Diego, 9500 Gilman Drive, La Jolla, CA 92093, USA

Abstract

The development of small-molecule inhibitors or stabilizers of selected protein–protein interactions (PPIs) of interest holds considerable promise for the development of research tools as well as candidate therapeutics. In this context, the covalent modification of selected residues within the target protein has emerged as a promising mechanism of action to obtain small-molecule modulators of PPIs with appropriate selectivity and duration of action. Different covalent labeling strategies are now available that can potentially allow for a rational, ground-up discovery and optimization of ligands as PPI inhibitors or stabilizers. This review article provides a synopsis of recent developments and applications of such tactics, with a particular focus on site-directed fragment tethering and proximity-enabled approaches.

Protein–protein interactions (PPIs) as viable targets in probe and drug discovery

PPIs contribute to a plethora of biological processes in both physiological and pathological conditions. For these reasons, different tactics and modalities, including small molecules, peptides, protein-therapeutics, and aptamers have been pursued to identify and develop modulators of selected PPIs of interest. In the realm of small molecules, which constitutes the focus of this review, the development of strategies that could facilitate the identification of PPI inhibitors or stabilizers continues to be the focus of intense research efforts. Whilst, historically, most research has been directed towards the development of PPI inhibitors, there is growing evidence that the stabilization of selected PPIs with small molecules is an

*Correspondence cballatore@health.ucsd.edu (C. Ballatore).

Declaration of interests

C.B. and K.R.F. are inventors in a patent application (#US Patent App. 17/611,036 pending to University of California and University of New Mexico) that covers HNA derivatives described in reference [25].

equally achievable and rewarding goal. In addition, although classical examples of clinically useful small molecule modulators of PPIs, such as taxanes and vinca alkaloids, have been known for a relatively long time (for example, the microtubule-stabilizing properties of paclitaxel were described in 1979 [1]), it was not until recently that an increasing number of PPIs have emerged as potentially tractable targets for small molecule drug and probe discovery programs [2]. This selection is even broader when considering those instances in which the particular PPI does not occur naturally, as is often seen in the case of **proteolysis-targeting chimera (PROTAC)** (see Glossary, Box 1) molecules, which are heterobifunctional constructs designed to induce a non-native interaction between two proteins [3].

In the context of small molecule modulators of PPIs, the targeted covalent modification (Box 2), either reversible or irreversible, of selected amino acid residue(s) has emerged as a promising strategy to attain adequate target engagement and duration of action. Although the covalent modification of proteins has been viewed with some concern, including the possible lack of selectivity and the appearance of idiosyncratic drug reactions, there has been renewed interest in this field over the past several years, fueled in part by the growing number of covalent drugs/drug candidates that are undergoing clinical development or that have reached regulatory approval [4,5]. Covalent labeling strategies were initially restricted to nucleophilic cysteine residues, however, there has been a significant expansion of the chemical strategies that could permit the covalent modification of other amino acid residues (for a recent comprehensive review on this topic see Grams and Hsu [6]).

Importantly, even though the identification of small-molecule modulators of PPIs has been largely the result of serendipitous discoveries, there is mounting evidence to indicate that different strategies can be utilized to effectively tackle PPIs in a more rational, ground-up fashion. Here, we focus on recent case studies that have utilized site-directed fragment tethering or proximity-enabled strategies and highlight the lessons learned.

Site-directed fragment tethering strategies

Site-directed approaches generally involve the optimization of a fragment-like molecule [i.e., molecular weight (MW) <250 Da] that can engage covalently within or in the proximity of a particular binding site of interest. In this context, the covalently bound fragment serves as an ‘anchor’ to which additional fragments can be appended (molecular growth) to occupy/fill a larger section of the site of interest and, thus, improve the overall complementarity of the final ligand with the target binding-site. Site-directed fragment-tethering approaches can be especially helpful to target challenging PPIs for which there are no known small-molecule ligands that could be considered as a starting point for analog design.

Disulfide tethering

‘Tethering’, a strategy originally developed by Wells and Erlanson [7], has been successfully exploited in fragment-based drug discovery programs [8,9] to identify low MW ligands (typically fragments of MW <250 Da) that interact with specific sites on proteins. Central to this site-directed strategy is the availability within the target site or its immediate

surroundings of a native or engineered cysteine residue, which is allowed to react reversibly with a library of disulfide-containing molecules, ultimately leading to the identification of the most stable complex.

The disulfide tethering approach has been recently used to identify fragments that stabilize the interaction between the 14-3-3σ protein and the phosphorylated motif of the breast cancer-associated transcription factor, estrogen receptor α (ERα) [10,11]. The 14-3-3 protein is a 'hub' protein that interacts with and regulates hundreds of protein partners [12,13], including promising targets like ERα for therapeutic development [13,14]. The natural product, fusicoccin A, suppresses ERα activity by virtue of its ability to stabilize the PPI between 14-3-3 and ERα. Therefore, stabilization of this PPI was proposed as a potentially attractive strategy to treat ERα-positive breast cancer. To that end, disulfide tethering (Figure 1A) was employed as a site-directed strategy to target the fusicoccin A binding site at the interface between 14-3-3 and ERα [10,15]. Of the seven different isoforms of 14-3-3, only the σ isoform exhibits a native, solvent-exposed cysteine residue, Cys^{38}, in the vicinity of the target site. Thus, this isoform and two other engineered protein constructs (i.e., one bearing Asn^{38} and Cys^{42}; and the other Asn^{38} and Cys^{45}) in which the Cys residues are closer to the binding site than Cys^{38}, were used to screen a library of 1600 disulfide fragments. The screen was performed with the proteins either in *apo* form or in complex with a 15-mer phosphopeptide comprising the 14-3-3-binding sequence of ERα. Selected fragments, **1** and **2** (Figure 1B), preferentially interacted with the protein–peptide complex over the *apo* form. Out of the three 14-3-3σ proteins (the native isoform and two engineered constructs), 14-3-3σ Cys^{42} resulted in the highest number of hits, which suggests optimal cysteine distance for fragment binding. In particular, for the 14-3-3σ Cys^{42} protein construct, fragment **2** exhibited the best cooperative binding as the efficiency of tethering increased from 26% in the case of the *apo* form to 60% for the protein–peptide complex. In addition, fragment **2** improved (i.e., decreased) the binding affinity constant (K_d) of the phosphopeptide for the 14-3-3σ Cys^{42} by 40-fold compared with the DMSO control. Interestingly, the co-crystal structures of the ternary complex revealed that the tethered fragment acts as a **molecular glue** by establishing interactions with both binding partners (Figure 1B) [10,16]. Further design of ligands that could cooperatively bind to the 14-3-3σ Cys^{42}/ERα complex included the exploration of the *para*- and *meta*-phenyl substitutions of **1** [16]. The PPI stabilization activity of each of the ligands was assessed by fluorescence anisotropy and the co-crystal structures of the ligand/14-3-3σ Cys^{42}/ERα ternary complexes were solved. These structures confirmed the cooperative binding of ligands with 14-3-3σ Cys^{42}/ERα [16].

Imine-based tethering

In an expansion of the disulfide-based tethering approach, fragments containing imine-forming aldehydes have been successfully deployed to reversibly engage the ε-amino group of selected noncatalytic lysine residues (Figure 1C). Compared with cysteine residues, lysines are considerably more abundant and their targeted modification would provide a more general platform to identify ligands for specific binding regions within proteins [17,18]. However, the pK_a of solvent-exposed lysine residues is ~10.4 [19], therefore, at physiologic pH, the fraction of the ε-amino group that is neutral and thus available

to react with electrophiles is approximately ~0.01%. Nonetheless, NMR studies have shown that appropriately substituted aromatic aldehydes, such as salicylaldehyde [20], and derivatives of *ortho*-formyl-phenylboronic acid [20,21], can efficiently establish reversible imine adducts with solvent-exposed lysines at physiologic pH.

Indeed, independent studies suggest that the aldimine chemistry (i.e., formation of imine adducts) is broadly applicable to site-directed fragment-tethering applications [22-25]. Wolter and co-workers first reported the use of imine-based tethering via aldehyde fragment screening in the context of the 14-3-3/NF-κβ PPI [24]. NF-κβ is a potential target in ischemia-reperfusion and breast cancer therapeutic interventions [26,27], however, targeting NF-κβ itself has been challenging and the modulation of the 14-3-3/NF-κβ PPI could be an alternative approach to targeting NF-κβ [28]. Aldehyde-bearing fragments were screened and evaluated for 14-3-3/NF-κβ binding (Figure 1D) using X-ray crystallography [24]. Several aromatic aldehydes that bind to Lys^{122} via aldimine formation were identified. All fragment hits featured electron-withdrawing groups around the aryl aldehyde, which suggests, at least in this case, the need for sufficiently activated aldehydes to efficiently generate the aldimine with Lys^{122}. One aryl aldehyde, which featured a *para*-sulfonamide group (**3**, Figure 1E), generated the highest affinity for the PPI and engaged in additional water-mediated contacts with the 14-3-3 Asn^{42} and Asp^{215}. The PPI stabilization was quantified via a fluorescence anisotropy assay, resulting in an apparent K_d of 1.1 μM, an eightfold improvement relative to the DMSO control [24].

A follow-up study further built on stabilizing the 14-3-3/NF-κβ PPI via imine-based tethering using an expanded library of aryl aldehydes [23]. In addition to the use of the previously identified hits, the available ligand/14-3-3/NF-κβ crystal structure complexes were utilized to identify potential binding sites surrounding the phosphorylation sites of the p65 subunit of NF-κβ, including potentially harnessing the p65 residues Ser^{45}, Ser^{281}, and Ser^{340}. A focused library of 2-, 3-, and 4-substituted benzaldehydes was first evaluated, followed by more comprehensive structure–activity relationship (SAR) studies using a larger library of 3-substitited and 4-nitrobenzaldehydes. One fragment, **4** (Figure 1F), was particularly promising due to the formation of additional interactions between the ligand and p65, including direct hydrophobic contacts with the Ile^{46} and Pro^{47} residues of p65. Interestingly, formation of the complex results in reorientation of the p65 peptide, leading to additional 14-3-3/p65 contacts and a consequent increase in the stability of the PPI. In addition to **4**, other sulfonamide analogs were developed, including **5** (Figure 1G), which improved stability by 81-fold relative to the DMSO control. Compound **5** was also assessed for selectivity against interactions between 14-3-3 and other protein binding partners. The data revealed that **5** is selective for the 14-3-3/p65 and is not a pan-stabilizer of other 14-3-3 interactions, likely due to the ligand's ability to reorient the 14-3-3/NF-κβ PPI (Figure 1G) [23].

Interestingly, the same imine-based tethering technique has also been exploited to identify stabilizers of the 14-3-3/Pin1 interaction [22]. Modulation of the 14-3-3/Pin1 PPI is of particular interest because of its role in the proteasomal degradation of the oncogene protein, Myc [29,30]. Evaluation of the 14-3-3/Pin1 interaction, including the use of co-crystal structures and computational studies, as well as fluorescent anisotropy studies, suggested

that the interaction occurs between the pSer^{72} site of Pin1 and the highly conserved Lys^{122} site of 14-3-3. A screening of 42 aldehyde fragments identified 11 fragments that stabilized the PPI. Three of these were *para*-imidazolyl aryl aldehydes (i.e., **6**, Figure 1H) that formed the intended aldimine with 14-3-3 Lys^{122}. Interestingly, all three fragments induced conformational changes in Pin1, making these fragments attractive starting points to developing selective cooperative binding ligands of the 14-3-3/Pin1 PPI. To further elucidate the SAR, hit fragments were grown by targeting the available space within the sub-pockets of Pin1. One ligand, **7** (Figure 1I), generated a 14-3-3/Pin1 PPI with an apparent K_d of 0.27 μM and a 96.8-fold enhancement relative to the DMSO control. The co-crystal structure of ligand **7** in complex with 14-3-3/Pin1 PPI (Figure 1I) revealed that the compound occupies a deep site formed by the 14-3-3 Cys^{38}, Arg^{41}, and Phe^{119}, which locks the orientation of the 2,4-difluoro ring. Importantly, ligand **7** led to a conformational change at the Asn^{42} site of 14-3-3, which facilitated the formation of a H-bond with the Gln^{75} of Pin1 as well as water-mediated H-bonds between the Trp^{75} and Gln^{75} of Pin1 and the Asn^{42} and Ser^{45} of 14-3-3. Several ligands, including **7**, were tested for selectivity utilizing a panel of 13 peptides that interact with 14-3-3. The data indicate that the compounds act selectively, as revealed by lack of significant stabilization of other 14-3-3/protein partner PPI models. Equally important, in the absence of protein partners, the ligands were neither significantly inhibitory nor effective in forming an aldimine with 14-3-3 Lys^{122} [22].

A different example of a site-directed, imine-based fragment-tethering is provided by the hydroxy-naphthaldehyde (HNA) fragment, which was identified as a *bona fide* inhibitor of a protein complex between the transmembrane protein, heart of glass1 (HEG1), and the Krev interaction trapped 1 (KRIT1) protein [25]. Both HEG1 and KRIT1, individually and through the formation of the PPI, play important roles in the regulation of Krüppel-like factors 4 and 2 (KLF4/2), which are important transcription factors that are implicated in endothelial vascular homeostasis [25,31,32]. Efforts to investigate the HEG1-KRIT1 PPI led to the identification of small-molecule inhibitors, such as the HNA derivatives. HNA was found to interfere with the HEG1-KRIT1 PPI by orthosterically competing with HEG1 via an imine bond with a noncatalytic lysine (Lys^{720}) of the FERM (4.1, ezrin, radixin, and moesin) domain of KRIT1 [25]. Structural analysis of the co-crystal structure of HNA bound within the HEG1-binding domain of KRIT1 identified a pocket in the proximity of the position 6 of the HNA scaffold (Figure 1J). Thus, substitution of the C6 position of the HNA with a methoxy group (**8**, Figure 1J) resulted in a derivative with improved inhibition of the PPI and in upregulation of KLF4/KLF2 in endothelial cells and in zebrafish [25].

Taken together, the aforementioned examples illustrate that the imine linkage could be broadly applicable as the directing tether. Also, the reversible nature of the imine adduct would allow for further optimization of the imine-forming fragment based on its ability to establish other favorable contacts within the binding site.

Proximity-enabled covalent strategies

Proximity-enabled covalent strategies generally require the availability of a noncovalent ligand for a particular protein/site of interest. The ligand is then typically modified to incorporate an electrophilic group which, depending on the application (*vide infra*), may

be an electrophilic cleavable linker (ECL), or a warhead, such as sulfonyl fluoride [33,34], thiocyanate [35], or an aldehyde-based warhead [20,36,37] that could potentially react with specific amino acid residues. Key to the success of proximity-enabled strategies is the identification of warheads of appropriate chemical reactivity, such that effective covalent modification of the target protein can be achieved without compromising chemical/metabolic stability. Examples of proximity-enabled covalent strategies discussed below include instances in which modification of the known noncovalent ligand resulted in congeners that could target specific amino acid residues in the proximity of the ligand binding site, leading to the formation of a stable covalent adduct. In addition, selected examples of ligand-directed chemistry for the labeling of a protein of interest (POI) with a reporter (e.g., fluorescent molecule or biotin), and covalent PROTACs are also discussed.

Ligand-directed chemistry

Ligand-directed chemistry has emerged as a protein labeling technique that harnesses ligand–protein affinity-based interactions to enable the covalent tagging of a POI [38,39]. The probe design involves a known ligand that has affinity for the POI, attached to a fluorescent or biotin reporter through an intervening ECL, such as tosyl, alkyloxyacyl imidazole, dibromophenylbenzoate, and *N*-acyl-*N*-alkyl sulfonamide (NASA) [40-46]. When the probe binds to the POI in a reversible manner, a nearby nucleophilic residue will attack the ECL, leading to the formation of a covalent adduct with the reporter and to the release of the ligand-linker fragment (Figure 2A). Among the different ECLs, the NASA may be particularly promising due to its favorable kinetics that allow for faster modification of the POI [46]. Using known ligands for model proteins, such as FK506-binding protein (FKBP12) and *Escherichia coli* dihydrofolate reductase (eDHFR), the kinetics and labeling efficiency of the NASA group have been evaluated and compared against other previously identified ECLs. The NASA group was found to label the target proteins rapidly and efficiently with rate constants of up to three orders of magnitude greater than other available chemistries (cf., NASA derivative, **9**, versus the corresponding alkyloxyacyl imidazole, **10**, and the dibromophenylbenzonate **11**, Figure 2B) [46].

To assess whether the rapid labeling was driven by the intrinsic reactivity of the NASA group or by the proximity effect caused by the affinity of the noncovalent ligand for the binding site, different ECL-based probes (**12**–**14**, Figure 2B) featuring either a low affinity (**12**) or a high affinity (**13**, **14**) FKBP12 ligand, were evaluated [46]. The data suggest that both the chemical reactivity of the NASA groups and the proximity effects caused by the noncovalent ligand play a critical role. Indeed, when comparing the binding kinetics of the high versus the low affinity NASA-based probes **13** and **12**, the former (high affinity) resulted in a 392-fold decrease in the rate constant relative to the latter (low affinity), illustrating the importance of the binding affinity of the ligand in promoting the desired alkylation event. However, a comparison of **13** with the high affinity but tosyl-based probe, **14**, shows a 644-fold faster protein labeling for the NASA-based compound (Figure 2B). While these results suggest that this strategy may be a broadly applicable protein-labeling technique, the same NASA-based ligand-directed approach could also be exploited to generate covalent ligands as candidate therapeutics. For example, the NASA group was utilized to design a covalent inhibitor of the heat shock protein 90 (Hsp90) using

an analog of a previously identified noncovalent inhibitor PU-H71 (**15**, Figure 2C) as a structural template [46]. In this case, the NASA-labeling strategy was first used to identify the covalently modifiable Lys^{58} close to the binding site [47]. Next, simple rearrangement of the NASA-linker group led to the covalent inhibitor, **16**, in which the NASA leaving group enables the covalent modification of Lys^{58} and the consequent irreversible inhibition of Hsp90 (Figure 2C). Compound **16** exhibited both strong binding affinity for Hsp90 ($K_i = 62$ nM) and cytotoxicity against SKBR3 tumor cells. In addition, consistent with the covalent interaction, the Hsp90 inhibitory effects of **16** were maintained even after repeated washing of the tumor cells [46].

Affinity enhancement through aldehyde-based warheads

In addition to the use of imine-based tethering for site-directed ligand development, imine-chemistry has also been used in affinity-based strategies. In particular, studies have examined whether the strategic incorporation of aldehyde-containing fragments in the structure of known noncovalent ligands may be used to selectively target lysine residues in the proximity of the binding site, leading to an overall enhancement of binding affinity. NMR studies revealed that certain aldehyde-containing fragments, such as the 2-hydroxybenzaldehydes and other aromatic aldehydes, can efficiently form imine adducts with *N*-α-acetyl-lysine at physiological pH without evidence of competing reactions (e.g., hydration of the aldehyde) [20]. An evaluation of the potential enhancement in binding affinity that may be attainable by incorporating these aryl aldehydes was assessed in the context of different proteins targets. Using a series of locked nucleic acids (LNAs) bound to known protein ligands (see general structures **17–19**, Figure 3A) and equipped with either an unsubstituted phenyl ring (**17**), or a benzaldehyde (**18**), or a 2-hydroxybenzaldehyde (**19**), the binding affinity of each of the constructs for the corresponding protein target [i.e., human serum albumin (HSA), human interleukin-2 (IL2), or bovine carbonic anhydrase II (CAII)] was evaluated. Except for constructs targeting CAII, the LNAs of general structure **19** that feature the 2-hydroxybenzaldehyde motif displayed the highest affinity for the target proteins, likely due to the higher efficiency in forming the imine adduct. Interestingly, the lack of affinity enhancement that was registered in the case of CAII may be explained with the lack of lysine residues in the vicinity of the CAII active site [20].

A similar approach has been applied in the context of inhibitors of urokinase-type plasminogen activator (uPa), a protein that is overexpressed in breast cancer [48]. Studies have shown that benzamidine, a broad-spectrum serine protease inhibitor, is a weak inhibitor of uPa with a K_d value of 180 μM [48]. Importantly, the Lys^{143} residue of uPa is in close proximity to the binding site and it was hypothesized that this residue might be targetable via aldimine chemistry. Several benzamidine congeners were synthesized, including an aldehyde-free derivative, (**20**), a benzaldehyde (**21**), and hydroxybenzaldehyde (**22**) derivatives (Figure 3B). Relative to **20** and **21**, compound **22** exhibited a 20-fold better potency [20]. These examples illustrate the utility of the 2-hydroxybenzaldehyde, among other benzaldehydes, as an efficient imine-forming moiety for ligand-directed affinity enhancement.

Although, as noted earlier, various reports have demonstrated that the aldimine chemistry can be successfully utilized to target lysine residues in protein targets [20,25,49], the imine adduct, if not adequately stabilized through intra- or intermolecular interactions, may undergo rapid hydrolysis that results in a rapid dissociation of the complex and, consequently, in a short duration of action. To improve the thermodynamic stability and prolong the residence time of the imine adduct, the use of a neighboring boronic acid group, which results in the formation of a stabilized iminoboronate (Figure 3C), has been explored [37,50,51]. In spite of its reversibility, the iminoboronate group exhibits a greater thermodynamic stability than its imine counterpart, which could result in a prolonged duration of protein labeling. A notable example showcasing the utility of iminoboronate-forming aryl boronic acid carbonyl warheads are small-molecule inhibitors of myeloid cell leukemia (Mcl-1) [21]. Mcl-1 is overexpressed in different tumors to neutralize proapoptotic proteins [52]. For this reason, numerous programs have been focusing on the development of small molecule inhibitors of Mcl-1 [53]. In one program, a known noncovalent ligand for Mcl-1 was modified by appending the aryl boronic acid carbonyl warhead into the structure of a known ligand (**24** and **25**, Figure 3D) [21]. These landmark proof-of-concept studies demonstrated that incorporating the iminoboronate chemistry into the noncovalent ligand resulted in an efficient targeting of the Lys^{234} of Mcl-1, with a consequent improvement in the biological activity as determined by biochemical assay. Notably, the activity of the constructs was also maintained in a cellular assay suggesting that the incorporation of the boronic acid warhead did not limit cell-entry.

In a further expansion of the iminoboronate chemistry, the diazaborine system (Figure 3C,E) provided an even greater degree of stabilization of the imine moiety compared with the iminoboronates [36]. To assess the efficiency of diazaborine formation relative to the iminoboronate, the binding kinetics was assessed using UV-vis and NMR spectroscopy. These studies revealed that the diazaborine exhibited a much longer residence time (7–16 hours) compared with the iminoboronate (estimated to be in milliseconds). Notably, the diazaborine warheads were evaluated in the context of inhibitors of *Staphylococcus aureus* sortase A (SrtA), a promising antibacterial target [54,55]. The cyclic peptide inhibitor, **26** (Figure 3E), was used as the starting ligand to which a (2-acetylphenyl)boronic acid (e.g., the iminoboronate-forming, **27**) or a diazaborine-forming benzaldehyde **28** were installed. In cell-free conditions, both **27** and **28** resulted in improved inhibition relative to **26** (Figure 3E) with 3.7- and 13-fold decreases in the IC_{50} values, respectively. In cell-based experiments, both **27** and **28** demonstrated comparable IC_{50} values of 3.7 and 2.9 μM, respectively. However, washout experiments revealed that **28** has a considerably longer-lasting inhibition activity compared with **27**, presumably due to its longer residence time [36].

Covalent PROTAC

With the resurgence of covalent drug discovery and the rapidly growing interest in PROTAC molecules (Box 1), the idea of merging these two methodologies has been investigated. Studies have focused on the development of PROTACs with covalent ligands to a particular POI that will recruit one of four widely used E3 ligases [i.e., cereblon (CRBN), Von Hippel-Lindau (VHL), inhibitor of apoptosis proteins (IAP), or mouse double minute 2

(MDM2)] [56]. Bruton's tyrosine kinase (BTK) is an important signaling protein in B cell lymphomas and has recently been used as a model system to develop covalent PROTACs [57]. Some of the most successful ligands for BTK are compounds that covalently modify a noncatalytic cysteine (Cys^{481}) in the active site, including the FDA approved drug, ibrutinib. The first attempt to build a covalent PROTAC utilized ibrutinib by coupling this compound with a variety of ligands and linkers for two different E3 ligases (e.g., **29**, Figure 4A) [58]. However, these early efforts did not produce the desired degradation of BTK [58]. In another study, several covalent PROTACs were designed, including those derived from ibrutinib and other covalent ligands of BTK (e.g., **30**, Figure 4A) [59]. These covalent PROTACs were designed to be irreversible covalent modifiers and, as a result, they were potentially suboptimal due to the loss of catalytic benefit of the reversible PROTACs [59]. However, recent studies reported reversible covalent PROTACs (Figure 4B) [60,61]. In this case, the PROTAC design involved the modulation of the electrophilicity and reversibility of the covalent warhead by implementing an α-cyano acrylamide, followed by the optimization of a variety of linkers to the CRBN ligand, pomalidomide (**31**, Figure 4B). The resulting PROTAC construct, **31**, degraded BTK in MOLM-14 cells with a half-maximal degradation concentration of 6.6 nM. Despite the suboptimal physicochemical properties caused by the high MW, a common problem with PROTAC constructs, **31** had high intracellular concentration and BTK occupancy. Importantly, when compared with its noncovalent derivative **32**, **31** caused considerably more BTK to degrade at lower concentrations, further highlighting the advantage of reversible covalent PROTACs [60]. This study illustrates the promise of the reversible covalent PROTACs in which the catalytic activity is retained.

Concluding remarks and future perspectives

There has been considerable progress in the development of covalent strategies that facilitate the discovery and optimization of small-molecule PPI modulators. The case studies presented here highlight a variety of strategies being used to develop small-molecule inhibitors or stabilizers for selected PPIs of interest. Particularly intriguing are the examples illustrating the discovery of PPI-stabilizing small molecules that exhibit binding cooperativity. However, notwithstanding the significant advances discussed, it seems likely that depending on the particular context and/or the approach used to identify small-molecule modulators of PPIs, additional challenges (see Outstanding questions), not least, the **developability** of candidate compounds will have to be addressed [62]. For example, with respect to the different covalent labeling strategies, several of the examples discussed here illustrate how the elaboration of the classical aldimine chemistry has resulted in promising fragment-tethering or proximity-enabled approaches. Although there is growing evidence to support the developability of aldehydes [63], including the recent approval of voxelotor (salicylic aldehyde warhead) to treat sickle cell disease [49], success is likely to be context-dependent. Also, the possible implications of incorporating the more elaborate iminoboronate- or diazaborine-forming fragments have not been thoroughly evaluated. Nonetheless, the expectation is that further exploration/application of these and other covalent labeling strategies will provide additional breakthroughs.

Acknowledgments

K.R.F. was supported by the CARING T32 Training Grant (T32AI007036).

Glossary

Activity-based protein profiling
a strategy to study the activity profiles of different enzyme and protein classes using chemical probes equipped with different covalent reactive groups.

Developability
term used to describe the likelihood that a candidate compound exhibits adequate characteristics for a successful progression through the drug development stages.

Molecular glue
a small molecule that interacts with two protein surfaces enhancing the affinity of the two proteins towards each other.

Proteolysis-targeting chimera (PROTAC)
heterobifunctional molecular constructs that bring a target protein and an E3 ligase together and induce target protein degradation.

Ubiquitin proteasome system (UPS)
a protein degradation system in eukaryotes that involves the sequential covalent attachment of ubiquitin proteins to the target protein by an E3 ligase. The ubiquitinylated protein is then recognized and degraded by the proteasome.

References

1. Schiff PB et al. (1979) Promotion of microtubule assembly in vitro by Taxol. Nature 277, 665–667 [PubMed: 423966]
2. Arkin MR et al. (2014) Small-molecule inhibitors of protein-protein interactions: progressing toward the reality. Chem. Biol 21, 1102–1114 [PubMed: 25237857]
3. Hughes SJ and Ciulli A (2017) Molecular recognition of ternary complexes: a new dimension in the structure-guided design of chemical degraders. Essays Biochem. 61, 505–516 [PubMed: 29118097]
4. Boike L. et al. (2022) Advances in covalent drug discovery. Nat. Rev. Drug Discov 21, 881–898 [PubMed: 36008483]
5. Singh J. (2022) The ascension of targeted covalent inhibitors. J. Med. Chem 65, 5886–5901 [PubMed: 35439421]
6. Grams RJ and Hsu KL (2022) Reactive chemistry for covalent probe and therapeutic development. Trends Pharmacol. Sci 43, 249–262 [PubMed: 34998611]
7. Erlanson DA et al. (2000) Site-directed ligand discovery. Proc. Natl. Acad. Sci. U. S. A 97, 9367–9372 [PubMed: 10944209]
8. Murray CW and Rees DC (2009) The rise of fragment-based drug discovery. Nat. Chem 1, 187–192 [PubMed: 21378847]
9. Erlanson DA et al. (2019) Fragment-based drug discovery: advancing fragments in the absence of crystal structures. Cell Chem. Biol 26, 9–15 [PubMed: 30482678]
10. Sijbesma E. et al. (2019) Site-directed fragment-based screening for the discovery of protein-protein interaction stabilizers. J. Am. Chem. Soc 141, 3524–3531 [PubMed: 30707565]

11. De Vries-van Leeuwen IJ et al. (2013) Interaction of 14-3-3 proteins with the estrogen receptor alpha F domain provides a drug target interface. Proc. Natl. Acad. Sci. U. S. A 110, 8894–8899 [PubMed: 23676274]
12. Pennington KL et al. (2018) The dynamic and stress-adaptive signaling hub of 14-3-3: emerging mechanisms of regulation and context-dependent protein-protein interactions. Oncogene 37, 5587–5604 [PubMed: 29915393]
13. Stevers LM et al. (2018) Modulators of 14-3-3 protein-protein interactions. J. Med. Chem 61, 3755–3778 [PubMed: 28968506]
14. Pair FS and Yacoubian TA (2021) 14-3-3 Proteins: novel pharmacological targets in neurodegenerative diseases. Trends Pharmacol. Sci 42, 226–238 [PubMed: 33518287]
15. Brink HJ et al. (2022) Fusicoccin-A targets cancerous inhibitor of protein phosphatase 2A by stabilizing a C-terminal interaction with 14-3-3. ACS Chem. Biol 17, 2972–2978 [PubMed: 36255265]
16. Sijbesma E. et al. (2021) Exploration of a 14-3-3 PPI pocket by covalent fragments as stabilizers. ACS Med. Chem. Lett 12, 976–982 [PubMed: 34136078]
17. Hacker SM et al. (2017) Global profiling of lysine reactivity and ligandability in the human proteome. Nat. Chem 9, 1181–1190 [PubMed: 29168484]
18. Abbasov ME et al. (2021) A proteome-wide atlas of lysine-reactive chemistry. Nat. Chem 13, 1081–1092 [PubMed: 34504315]
19. Grimsley GR et al. (2009) A summary of the measured pK values of the ionizable groups in folded proteins. Protein Sci. 18, 247–251 [PubMed: 19177368]
20. Dal Corso A et al. (2018) Affinity enhancement of protein ligands by reversible covalent modification of neighboring lysine residues. Angew. Chem. Int. Ed. Engl 57, 17178–17182 [PubMed: 30398299]
21. Akçay G. et al. (2016) Inhibition of Mcl-1 through covalent modification of a noncatalytic lysine side chain. Nat. Chem. Biol 12, 931–936 [PubMed: 27595327]
22. Cossar PJ et al. (2021) Reversible covalent imine-tethering for selective stabilization of 14-3-3 hub protein interactions. J. Am. Chem. Soc 143, 8454–8464 [PubMed: 34047554]
23. Wolter M. et al. (2021) An exploration of chemical properties required for cooperative stabilization of the 14-3-3 interaction with NF-kappaB-utilizing a reversible covalent tethering approach. J. Med. Chem 64, 8423–8436 [PubMed: 34076416]
24. Wolter M. et al. (2020) Fragment-based stabilizers of protein-protein interactions through imine-based tethering. Angew. Chem. Int. Ed. Engl 59, 21520–21524 [PubMed: 32816380]
25. Lopez-Ramirez MA et al. (2021) Inhibition of the HEG1–KRIT1 interaction increases KLF4 and KLF2 expression in endothelial cells. FASEB BioAdv. 3, 334–355 [PubMed: 33977234]
26. Zhou XY et al. (2017) 14-3-3 Isoforms differentially regulate NFκB signaling in the brain after ischemia-reperfusion. Neurochem. Res 42, 2354–2362 [PubMed: 28424948]
27. Inglés-Esteve J. et al. (2012) Inhibition of specific NF-κB activity contributes to the tumor suppressor function of 14-3-3σ in breast cancer. PLoS One 7, e38347 [PubMed: 22675457]
28. Wolter M. et al. (2020) Selectivity via cooperativity: preferential stabilization of the p65/14-3-3 interaction with semisynthetic natural products. J. Am. Chem. Soc 142, 11772–11783 [PubMed: 32501683]
29. Phan L. et al. (2015) The cell cycle regulator 14-3-3σ opposes and reverses cancer metabolic reprogramming. Nat. Commun 6, 7530 [PubMed: 26179207]
30. Wen Y-Y et al. (2013) DNA damage-mediated c-Myc degradation requires 14-3-3 sigma. Cancer Hallm. 1, 3–17
31. Kleaveland B. et al. (2009) Regulation of cardiovascular development and integrity by the heart of glass-cerebral cavernous malformation protein pathway. Nat. Med 15, 169–176 [PubMed: 19151727]
32. Donat S. et al. (2018) Heg1 and Ccm1/2 proteins control endocardial mechanosensitivity during zebrafish valvulogenesis. Elife 7, e28939 [PubMed: 29364115]
33. Li Q. et al. (2020) Developing covalent protein drugs via proximity-enabled reactive therapeutics. Cell 182, 85–97 [PubMed: 32579975]

34. Zhang B. et al. (2023) Proximity-enabled covalent binding of IL-2 to IL-2Ralpha selectively activates regulatory T cells and suppresses autoimmunity. Signal Transduct. Target. Ther 8, 28 [PubMed: 36690610]
35. Ortiz Zacarias NV et al. (2021) Design and characterization of an intracellular covalent ligand for CC chemokine receptor 2. J. Med. Chem 64, 2608–2621 [PubMed: 33600174]
36. Reja RM et al. (2022) Lysine-targeting reversible covalent inhibitors with long residence time. J. Am. Chem. Soc 144, 1152–1157 [PubMed: 35040658]
37. Cal PM et al. (2012) Iminoboronates: a new strategy for reversible protein modification. J. Am. Chem. Soc 134, 10299–10305 [PubMed: 22642715]
38. Chen G. et al. (2003) Reactivity of functional groups on the protein surface: development of epoxide probes for protein labeling. J. Am. Chem. Soc 125, 8130–8133 [PubMed: 12837082]
39. Sakamoto S and Hamachi I (2023) Ligand-directed chemistry for protein labeling for affinity-based protein analysis. Isr. J. Chem 63, e202200077
40. Fujishima SH et al. (2012) Ligand-directed acyl imidazole chemistry for labeling of membrane-bound proteins on live cells. J. Am. Chem. Soc 134, 3961–3964 [PubMed: 22352855]
41. Wakayama S. et al. (2017) Chemical labelling for visualizing native AMPA receptors in live neurons. Nat. Commun 8, 14850 [PubMed: 28387242]
42. Yamaura K. et al. (2016) Discovery of allosteric modulators for GABAA receptors by ligand-directed chemistry. Nat. Chem. Biol 12, 822–830 [PubMed: 27526031]
43. Tsukiji S. et al. (2009) Ligand-directed tosyl chemistry for protein labeling in vivo. Nat. Chem. Biol 5, 341–343 [PubMed: 19330012]
44. Tamura T. et al. (2012) Native FKBP12 engineering by ligand-directed tosyl chemistry: labeling properties and application to photo-cross-linking of protein complexes in vitro and in living cells. J. Am. Chem. Soc 134, 2216–2226 [PubMed: 22220821]
45. Tamura T. et al. (2013) Fluorophore labeling of native FKBP12 by ligand-directed tosyl chemistry allows detection of its molecular interactions in vitro and in living cells. J. Am. Chem. Soc 135, 6782–6785 [PubMed: 23611728]
46. Tamura T. et al. (2018) Rapid labelling and covalent inhibition of intracellular native proteins using ligand-directed N-acyl-N-alkyl sulfonamide. Nat. Commun. 9, 1870 [PubMed: 29760386]
47. Immormino RM et al. (2006) Structural and quantum chemical studies of 8-aryl-sulfanyl adenine class Hsp90 inhibitors. J. Med. Chem 49, 4953–4960 [PubMed: 16884307]
48. Renatus M. et al. (1998) Structural and functional analyses of benzamidine-based inhibitors in complex with trypsin: implications for the inhibition of factor Xa, tPA, and urokinase. J. Med. Chem 41, 5445–5456 [PubMed: 9876114]
49. Oksenberg D. et al. (2016) GBT440 increases haemoglobin oxygen affinity, reduces sickling and prolongs RBC half-life in a murine model of sickle cell disease. Br. J. Haematol 175, 141–153 [PubMed: 27378309]
50. van der Zouwen AJ et al. (2021) Iminoboronates as dualpurpose linkers in chemical probe development. Chem. Eur. J 27, 3292–3296 [PubMed: 33259638]
51. Bandyopadhyay A and Gao J (2015) Iminoboronate formation leads to fast and reversible conjugation chemistry of α-nucleophiles at neutral pH. Chem. Eur. J 21, 14748–14752 [PubMed: 26311464]
52. Gores GJ and Kaufmann SH (2012) Selectively targeting Mcl-1 for the treatment of acute myelogenous leukemia and solid tumors. Genes Dev. 26, 305–311 [PubMed: 22345513]
53. Wang H. et al. (2021) Targeting MCL-1 in cancer: current status and perspectives. J. Hematol. Oncol 14, 67 [PubMed: 33883020]
54. Schneewind O and Missiakas D (2019) Sortases, surface proteins, and their roles in *Staphylococcus aureus* disease and vaccine development. Microbiol. Spectr 7. 10.1128/microbiolspec.PSIB-0004-2018
55. Zong Y. et al. (2004) Crystal structures of *Staphylococcus aureus* sortase A and its substrate complex. J. Biol. Chem 279, 31383–31389 [PubMed: 15117963]
56. Bricelj A. et al. (2021) E3 ligase ligands in successful PROTACs: an overview of syntheses and linker attachment points. Front. Chem 9, 707317 [PubMed: 34291038]

57. Grimster NP (2021) Covalent PROTACs: the best of both worlds? RSC Med. Chem 12, 1452–1458 [PubMed: 34671730]
58. Tinworth CP et al. (2019) PROTAC-mediated degradation of Bruton's tyrosine kinase is inhibited by covalent binding. ACS Chem. Biol 14, 342–347 [PubMed: 30807093]
59. Xue G. et al. (2020) Protein degradation through covalent inhibitor-based PROTACs. Chem. Commun 56, 1521–1524
60. Guo WH et al. (2020) Enhancing intracellular accumulation and target engagement of PROTACs with reversible covalent chemistry. Nat. Commun 11, 4268 [PubMed: 32848159]
61. Gabizon R. et al. (2020) Efficient targeted degradation via reversible and irreversible covalent PROTACs. J. Am. Chem. Soc 142, 11734–11742 [PubMed: 32369353]
62. Lu H. et al. (2020) Recent advances in the development of protein-protein interactions modulators: mechanisms and clinical trials. Signal Transduct. Target. Ther 5, 213 [PubMed: 32968059]
63. Gampe C and Verma VA (2020) Curse or cure? A perspective on the developability of aldehydes as active pharmaceutical ingredients. J. Med. Chem 63, 14357–14381 [PubMed: 32916044]
64. Kleiger G and Mayor T (2014) Perilous journey: a tour of the ubiquitin-proteasome system. Trends Cell Biol. 24, 352–359 [PubMed: 24457024]
65. Konstantinidou M. et al. (2019) PROTACs- a game-changing technology. Expert Opin. Drug. Discov 14, 1255–1268 [PubMed: 31538491]
66. Sun X. et al. (2019) PROTACs: great opportunities for academia and industry. Signal Transduct. Target. Ther 4, 64 [PubMed: 31885879]
67. Strelow JM (2017) A perspective on the kinetics of covalent and irreversible inhibition. SLAS Discov. 22, 3–20 [PubMed: 27703080]
68. Miyahisa I. et al. (2015) Rapid determination of the specificity constant of irreversible inhibitors (kinact/KI) by means of an endpoint competition assay. Angew. Chem. Int. Ed. Engl 54, 14099–14102 [PubMed: 26426864]
69. Bauer RA (2015) Covalent inhibitors in drug discovery: from accidental discoveries to avoided liabilities and designed therapies. Drug Discov. Today 20, 1061–1073 [PubMed: 26002380]
70. De Cesco S. et al. (2017) Covalent inhibitors design and discovery. Eur. J. Med. Chem 138, 96–114 [PubMed: 28651155]
71. Fang H. et al. (2021) Recent advances in activity-based probes (ABPs) and affinity-based probes (A*f*BPs) for profiling of enzymes. Chem. Sci 12, 8288–8310 [PubMed: 34221311]
72. Mons E. et al. (2022) A comprehensive guide for assessing covalent inhibition in enzymatic assays illustrated with kinetic simulations. Curr. Protoc 2, e419 [PubMed: 35671150]
73. Copeland RA (2016) The drug-target residence time model: a 10-year retrospective. Nat. Rev. Drug Discov 15, 87–95 [PubMed: 26678621]
74. Paramore A and Frantz S (2003) Bortezomib. Nat. Rev. Drug Discov 2, 611–612 [PubMed: 12908468]

Box 1.

Proteolysis targeting chimeras (PROTACs)

PROTACs are heterobifunctional molecules that are used to degrade aberrant proteins of interest (POIs). PROTACs utilize the **ubiquitin proteasome system (UPS)** to degrade the target protein. The UPS is one of the main pathways for the degradation of intracellular proteins, whereby proteins are marked for degradation by the covalent attachment of a chain of 76 amino acid-proteins called ubiquitin. Ubiquitination is a sequential process achieved by three enzyme classes: ubiquitin-activating enzymes (E1), ubiquitin conjugating enzymes (E2), and ubiquitin ligases (E3). The first step is the ATP-dependent activation and formation of a thioester bond between the carboxyl terminus of ubiquitin and the active site cysteine of E1. This activated ubiquitin is then transferred to E2. The final transfer of ubiquitin to the substrate protein from E2 is catalyzed by an E3 ubiquitin ligase before the process is repeated. The polyubiquitinated protein is then recognized by the proteasome for degradation [64]. PROTACs consist of a ligand for the POI connected to a ligand for an E3 ligase by an intervening linker (Figure I). The PROTAC induces a ternary complex between the POI and E3 ligase and, by proximity, induces ubiquitination of the POI and its subsequent degradation by the proteasome [65]. In this regard, PROTACs do not rely on the POI ligand occupying a binding site for its mechanism of action; the ligand can form a transient interaction with the POI that would initiate its degradation. This is advantageous for targeting proteins that lack well-defined binding sites (e.g., transcription factors) and for interfaces of PPIs [66]. Also, because the mechanism of action involves degradation of the target protein rather than occupancy and inhibition, PROTACs tend to have a long-lasting biological effect as the recovery of protein function is only attained through protein resynthesis [66].

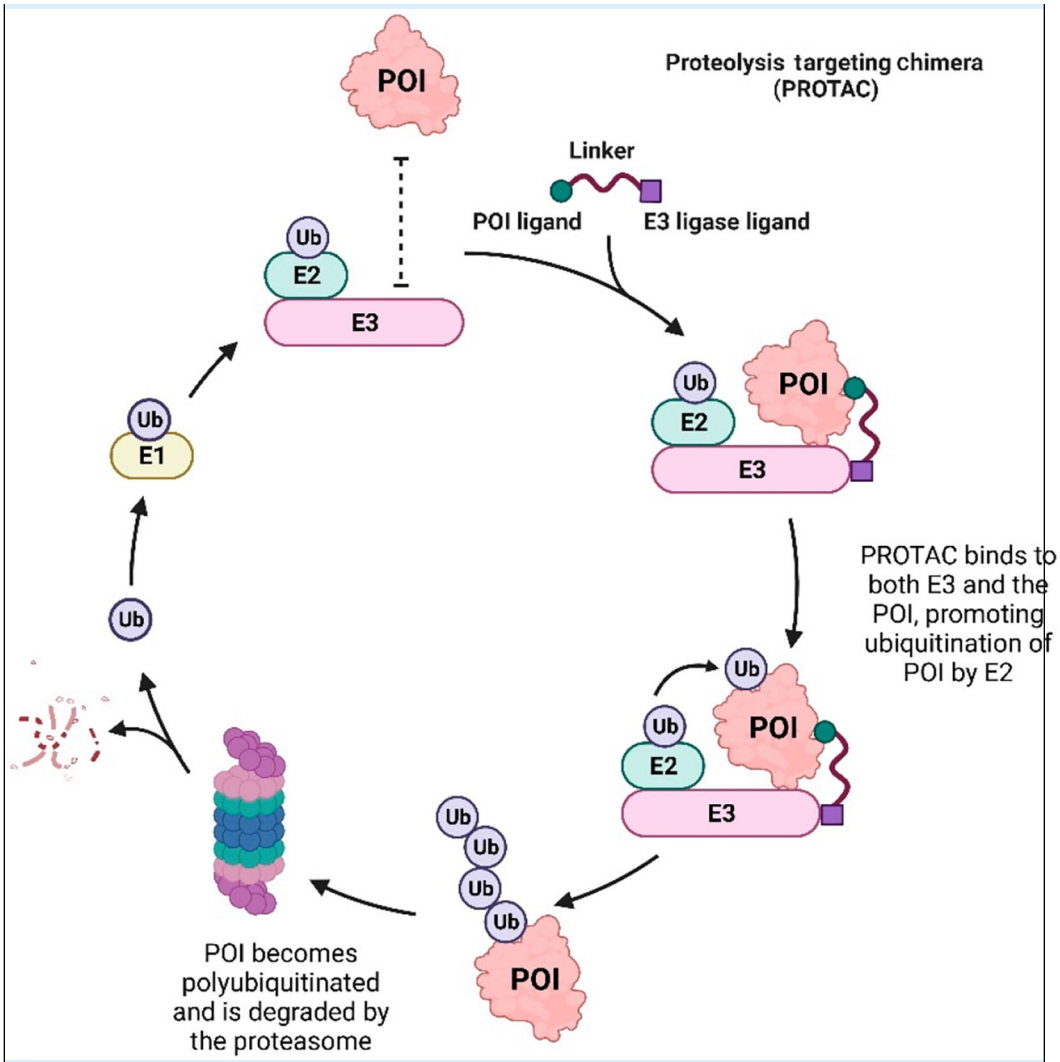

Figure I. General mechanism of proteolysis targeting chimeras (PROTACs). Figure created with BioRender.com.

Abbreviation: POI, protein of interest.

Box 2.

Kinetics of covalent ligands

Targeted covalent ligands (TCLs) are molecules equipped with electrophilic groups (warheads) that can covalently modify nucleophilic residues within the target protein, leading to the formation of relatively stable complexes [67,68]. Although the intrinsic chemical reactivity of electrophilic warheads may be problematic in terms of metabolic stability and/or off-target interactions [69], covalent ligands have found clinical success for a variety of indications [70]. In addition to their success as ligands for small molecule drug discovery, irreversible TCLs, which involve the formation of irreversible covalent bonds, have also found utility as chemical probes, specifically in the **activity-based protein profiling** of proteases, kinases, serine hydrolases, phosphatases, deacetylases, and cytochrome P450s [71]. Reversible TCLs, which involve the formation of reversible covalent bonds, are also advantageous due to their ability to form tight-complexes without permanently modifying the target or other off-target proteins. Because of the time-dependence of the covalent bond formation, an evaluation of binding kinetics is often an important aspect when assessing TCLs [67,72]. Typically, the binding kinetics follow a two- or one-step binding model [67,72,73]. For irreversible two-step binding kinetics (Equation 1), the initial noncovalent protein–ligand (PL) complex (first step) is followed by the formation of the covalent and irreversible bond (second step) and together these are defined by the rate constant k_{inact} / K_i [67,68]. In a reversible two-step binding model, the first step also involves the formation of the noncovalent PL complex, but in this case is followed by the formation of a reversible covalent PL^* complex, both of which are measured using the equilibrium constant, K_i^* (Equation 2) [73]. One-step covalent inhibition, which involves the formation of the covalent PL^* complex without the initial, noncovalent interaction, can also be observed for both irreversible (Equation 3) and reversible (Equation 4) covalent ligands [67,73]. Although one-step covalent inhibition is considered less desirable due to it often being indicative of high intrinsic chemical reactivity, one-step covalent inhibitors have found clinical success, such as in the case of anticancer drug, bortezomib (Velcade®) [74]. Development of covalent ligands typically involve the optimization of kinetic parameters, including the on rate (k_1), the off rate (k_2), and, for covalent reversible ligands, the residence time [73].

$$P + L \underset{k_2}{\overset{k_1}{\rightleftharpoons}} PL \xrightarrow{k_{inact}} PL^* \qquad K_i = \frac{[P][L]}{[PL]} = K_i + \frac{k_{inact}}{k_1} \qquad \text{Two} - \text{step, irreversible}$$

[I]

$$P + L \underset{k_2}{\overset{k_1}{\rightleftharpoons}} PL \underset{k_4}{\overset{k_3}{\rightleftharpoons}} PL^* \qquad K_i^* = \frac{[P][L]}{[PL] + [PL^*]} = \frac{K_i}{1 + \frac{k_3}{k_4}} \qquad \text{Two} - \text{step, reversible}$$

[II]

$$P + L \xrightarrow{k_{chem}} PL^* \qquad \text{One-step, irreversible} \qquad \text{[III]}$$

$$P + L \underset{k_2}{\overset{k_1}{\rightleftharpoons}} PL^* \qquad K_i = \frac{[P][L]}{[PL]} = \frac{k_2}{k_1} \qquad \text{One} - \text{step, reversible} \qquad \text{[IV]}$$

Where $P + L$ are the unbound protein and ligand; PL, noncovalent complex; PL^*, covalent complex; K_i and K_i^*, equilibrium constants; K_i, inactivation constant; k_{inact}, maximum rate of inactivation; k_{chem}, inactivation potency.

Outstanding questions

Can existing computational prediction tools be used or optimized to efficiently predict binding cooperativity in the context of PPI stabilization?

Imine-based fragment tethering approaches may offer potential advantages compared, for example, with already very successful disulfide fragment tethering. However, further studies are clearly needed to fully evaluate the potential of this strategy.

Iminoboronate and diazaborine can efficiently engage the ε-amino group of noncatalytic lysines. However, the possible impact that these fragments may have on the overall ADME-PK and physicochemical properties of the ligand will have to be examined.

Highlights

Whereas, historically, the majority of efforts toward small-molecule modulators of PPIs have largely focused on PPI inhibitors, there is growing evidence that stabilization of selected PPIs with small molecules is an achievable goal.

Targeted covalent modification of amino acid residues within proteins of interest is a validated strategy that has the potential of providing both selectivity and duration of action.

Different covalent labeling strategies have been developed that can facilitate the identification of small-molecule modulators of PPIs.

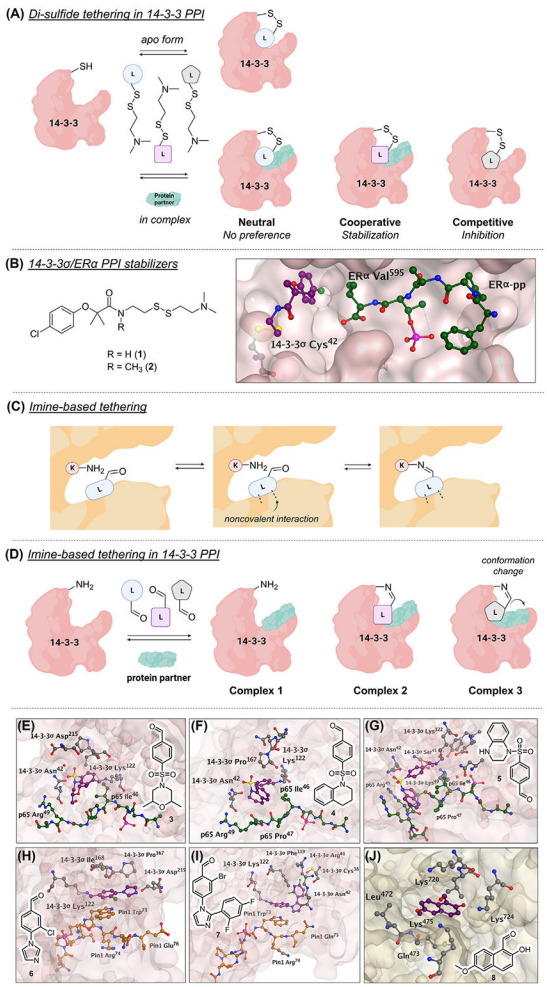

Figure 1. Site-directed approaches.

(A) Outline of the disulfide tethering approach utilized to screen for stabilizers of the 14-3-3σ/ERα protein–protein interaction (PPI). A library of disulfide fragments was screened and tethering was determined via mass spectrometry. Fragments were classified as neutral (no preference for either the PPI or the *apo* form), cooperative (preference for the PPI complex), or competitive (only binding to the *apo*-14-3-3). (B) Chemical structures of 14-3-3σ/ERα PPI stabilizers **1** and **2**. The co-crystal structure of **1** bound to the 14-3-3σ/ERα complex provided insight into the compound's mechanism of PPI stabilization by revealing both the formation of a disulfide bond with the 14-3-3σ Cys^{42} and hydrophobic contacts between the *para*-phenyl of **1** and the C-terminal Val^{595} of ERα [Protein Data Bank (PDB): 6HMT]. (C) Outline of the imine-based tethering approach. (D) Imine-based tethering in the 14-3-3 hub protein utilizes the native 14-3-3 Lys^{122}, which is located near several known 14-3-3 binding partners (Complex 1). Screening efforts with aldehyde libraries identified aromatic aldehydes capable of forming aldimines with 14-3-3 Lys^{122} and cooperatively bind with the protein partner (ERα and Pin1; Complex 2). Ligands that cooperatively bind the PPI and induce conformational change increase PPI stability and selectivity (Complex 3). Co-crystal structures of PPI stabilizers, **3** (E) PDB: 6YQ2, **4** (F) PDB: 7NJ9, and **5** (G) PDB: 7BIW, bound to the 14-3-3 (pink surface)/ERα (green)

PPI. Co-crystal structures of 14-3-3/Pin1 (orange) PPI stabilizers, **6** (H) PDB: 7AXN and **7** (I) PDB: 7BFW. (J) Co-crystal structure of the HEG1-KRIT1 (yellow surface) inhibitor, **8**, bound to KRIT1 (PDB: 6UZK). Figure (A, C, D) created with BioRender.com.

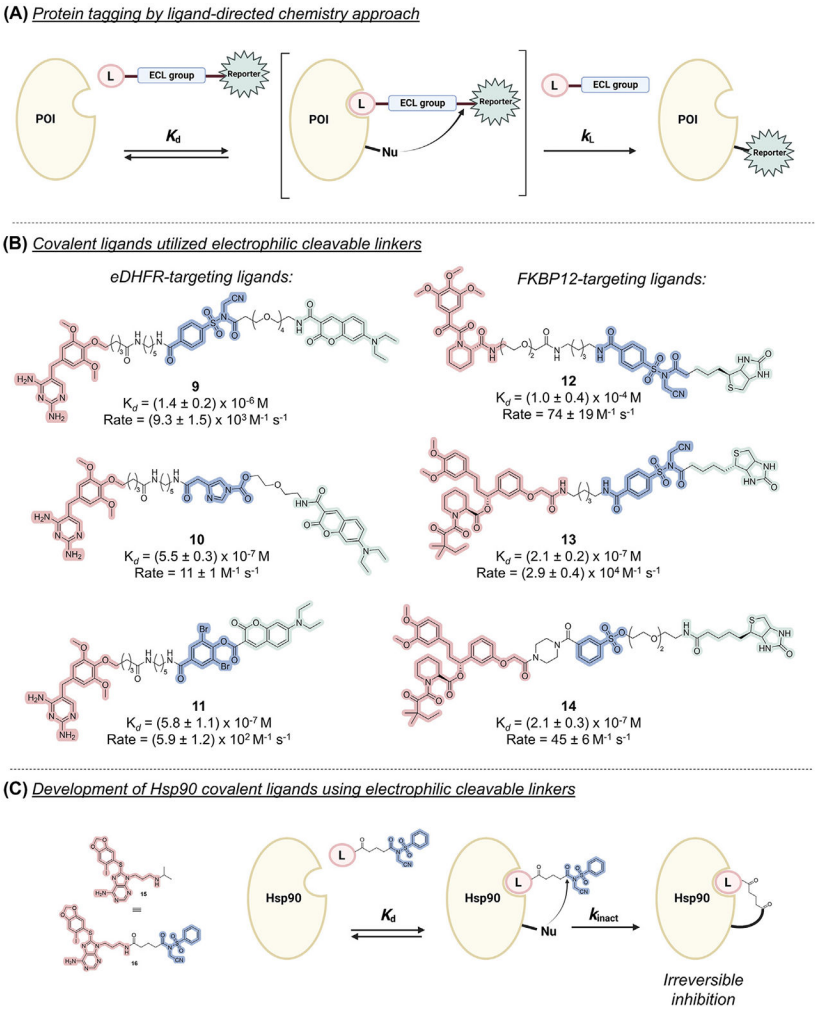

Figure 2. Ligand-directed chemistry approach.

(A) General mechanism of protein tagging by the ligand-directed chemistry approach. (B) Covalent ligands utilizing electrophilic cleavable linkers and their binding affinity and kinetics in *Escherichia coli dihydrofolate reductase (*eDHFR) or FK506-binding protein (FKBP12). Binding affinity and kinetics were determined by matrix-assisted laser desorption/ionization time-of-flight mass spectrometry (MALDI-TOF MS) [46]. (C) An irreversible covalent inhibitor of Hsp90 was developed utilizing electrophilic cleavable linker (ECL). Figure (A, C) created with BioRender.com. Abbreviation: POI, protein of interest.

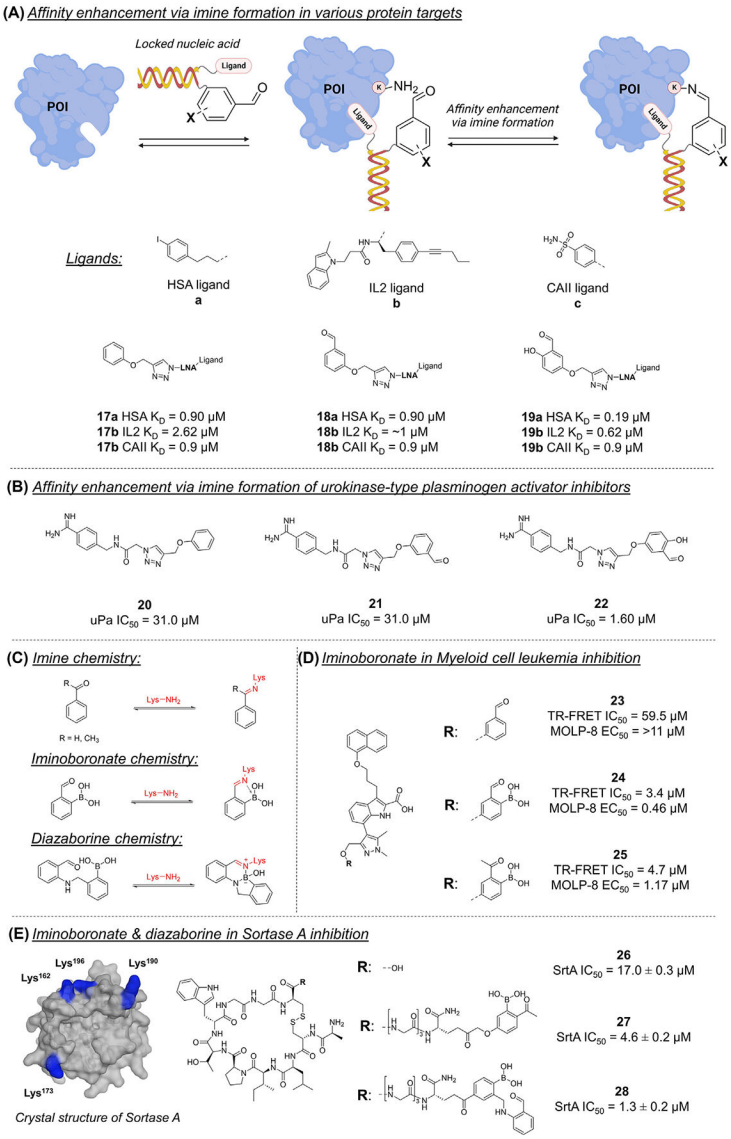

Figure 3. Other examples of proximity-enabled covalent strategies.

(A) Affinity enhancement of locked nucleic acid (LNA) ligands via imine formation with a lysine residue in the vicinity of the ligand binding site, the structures of known ligands for the target proteins, and the binding affinities of aldehyde-based LNAs to their respective targets. Binding affinities were determined by fluorescence polarization (FP) assay. (B) Urokinase-type plasminogen activator (uPa) inhibition activity of benzamidine derivatives as determined by enzymatic inhibition assay. (C) Summary of imine chemistries, including the stabilization by iminoboronate and diazaborine. (D) Imine-forming Mcl-1 inhibitors, including aldehyde **23** and iminoboronate-forming **24** and **25**. TR-FRET IC_{50} values are in cell-free conditions. Mcl-1-dependent multiple myeloma (MOLP-8) EC_{50} values represent the caspase activity in MOLP-8 cells. (E) Crystal structure of *Staphylococcus aureus* SrtA (Protein Data Bank: 1T2W) indicates the presence of several lysine residues (blue) near the binding site. Srt A is inhibited by cyclic peptide **26** and appending an iminoboronate (**27**) or a diazaborine (**28**) forming warhead resulted in improved inhibition. The IC_{50} values shown

are from cell-free conditions. Figure (A) created with BioRender.com. Abbreviations: CAII, bovine carbonic anhydrase II; HAS, human serum albumin; IL2, human interleukin-2.

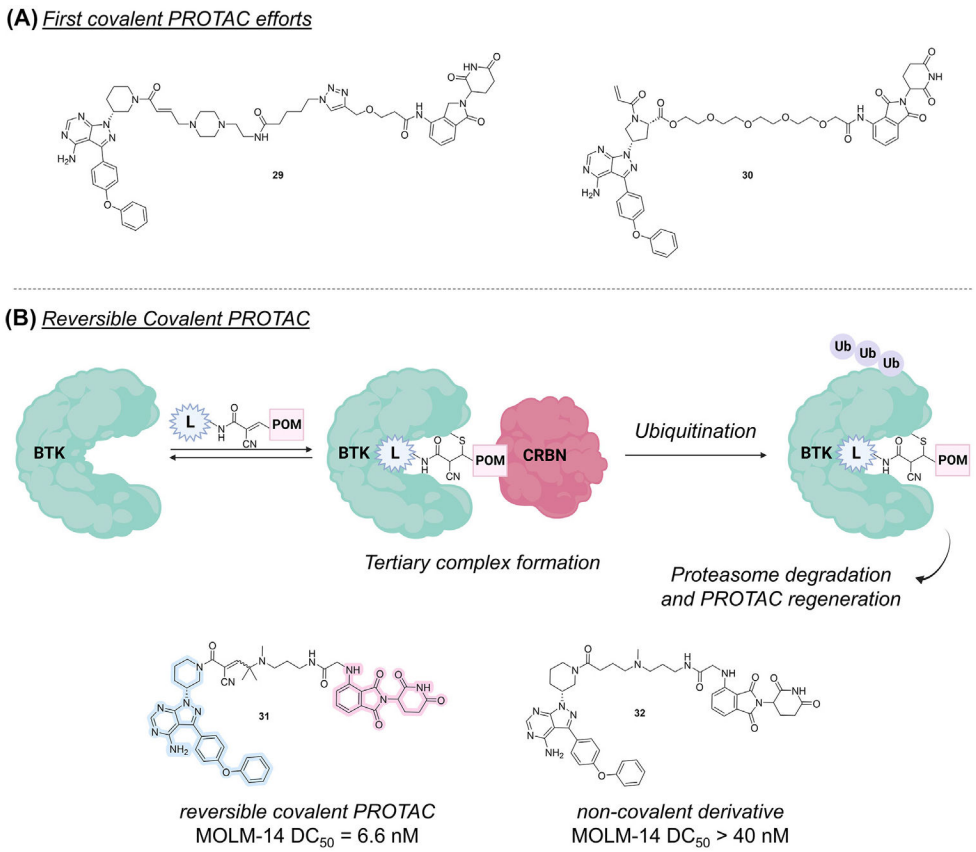

Figure 4. Covalent proteolysis targeting chimeras (PROTACs).

(A) Examples of covalent PROTACs, including a first unsuccessful attempt (**29**) and an irreversible PROTAC (**30**). (B) A reversible covalent PROTAC (**31**), including its mechanism of action that involves the formation of a thioether between **31** and Bruton's tyrosine kinase (BTK) Cys^{481}. PROTAC structure: BTK ligand (blue), the known cereblon (CRBN) ligand pomalidomide (pink), and the pomalidomide with linker (POM). The noncovalent analog, **32**, resulted in loss of activity. MOLM-14 half-maximal degradation concentration (DC_{50}) values represent BTK degradation in MOLM-14 cells. Figure (B) created with BioRender.com.